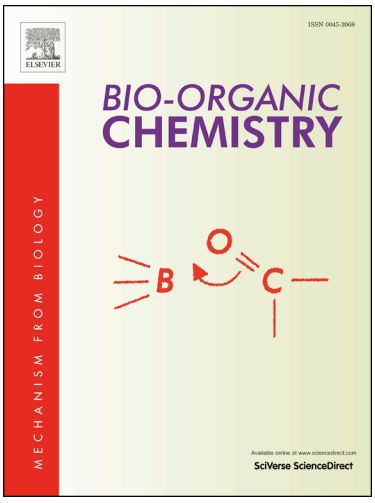

Design, synthesis, docking study, α-glucosidase inhibition, and cytotoxic activities of acridine linked to thioacetamides as novel agents in treatment of type 2 diabetes

Maryam Mohammadi-Khanaposhtani, Sepideh Rezaei, Reza Khalifeh, Somaye Imanparast, Mohammad Ali Faramarzi, Saeed Bahadorikhalili, Malihe Safavi, Fatemeh Bandarian, Ensieh Nasli Esfahani, Mohammad Mahdavi, Bagher Larijani

PII: S0045-2068(18)30251-7
DOI: https://doi.org/10.1016/j.bioorg.2018.06.035
Reference: YBIOO 2415

To appear in: *Bioorganic Chemistry*

Received Date: 14 March 2018
Revised Date: 17 June 2018
Accepted Date: 29 June 2018

Please cite this article as: M. Mohammadi-Khanaposhtani, S. Rezaei, R. Khalifeh, S. Imanparast, M. Ali Faramarzi, S. Bahadorikhalili, M. Safavi, F. Bandarian, E. Nasli Esfahani, M. Mahdavi, B. Larijani, Design, synthesis, docking study, α-glucosidase inhibition, and cytotoxic activities of acridine linked to thioacetamides as novel agents in treatment of type 2 diabetes, *Bioorganic Chemistry* (2018), doi: https://doi.org/10.1016/j.bioorg.2018.06.035

Design, synthesis, docking study, α-glucosidase inhibition, and cytotoxic activities of acridine linked to thioacetamides as novel agents in treatment of type 2 diabetes

Maryam Mohammadi-Khanaposhtani [a], Sepideh Rezaei [b], Reza Khalifeh [b], Somaye Imanparast [c], Mohammad Ali Faramarzi [c], Saeed Bahadorikhalili [d], Malihe Safavi [e], Fatemeh Bandarian [f], Ensieh Nasli Esfahani [f], Mohammad Mahdavi [f, *], Bagher Larijani [f, *]

[a] *Cellular and Molecular Biology Research Center, Health Research Institute, Babol University of Medical Sciences, Babol, Iran*

[b] *Department of Chemistry, Shiraz University of Technology, Shiraz, Iran*

[c] *Department of Pharmaceutical Biotechnology, Faculty of Pharmacy and Biotechnology Research Center, Tehran University of Medical Sciences, Iran*

[d] *School of Chemistry, College of Science, University of Tehran, Tehran, Iran*

[e] *Department of Biotechnology, Iranian Research Organization for Science and Technology (IROST), Tehran, Iran*

[f] *Endocrinology and Metabolism Research Center, Endocrinology and Metabolism Clinical Sciences Institute, Tehran University of Medical Sciences, Tehran, Iran*

Abstract:

A novel series of acridine linked to thioacetamides **9a–o** were synthesized and evaluated for their α-glucosidase inhibitory and cytotoxic activities. All the synthesized compounds exhibited excellent α-glucosidase inhibitory activity in the range of IC_{50} = 80.0 ± 2.0–383.1 ± 2.0 μM against yeast α-glucosidase, when compared to the standard drug acarbose (IC_{50} = 750.0 ± 1.5 μM). Among the synthesized compounds, 2-((6-chloro-2-methoxyacridin-9-yl)thio)-*N*-(p-tolyl) acetamide **9b** displayed the highest α-glucosidase inhibitory activity (IC_{50} = 80.0 ± 2.0 μM). The *in vitro* cytotoxic assay of compounds **9a–o** against MCF-7 cell line revealed that only the compounds **9d**, **9c**, and **9n** exhibited cytotoxic activity. Cytotoxic compounds **9d**, **9c**, and **9n** did not show cytotoxic activity against the normal human cell lines HDF. Kinetic study revealed that

the most potent compound **9b** is a competitive inhibitor with a K_i of 85 μM. Furthermore, the interaction modes of the most potent compounds **9b** and **9f** with α-glucosidase were evaluated through the molecular docking studies.

Key words: α-Glucosidase; Type 2 diabetes; Acridine; Thioacetamide; Docking study

1. Introduction

α-Glucosidase leads to the breakdown of oligo- and disaccharides from dietary complex carbohydrates. Inhibition of this enzyme reduced the absorption of monosaccharides and control of postprandial glucose level [1]. Several α-glucosidase inhibitors such as acarbose, voglibose, and miglitol are approved for the treatment of type 2 diabetes [2-4]. In addition, certain evidences suggest that α-glucosidase inhibitors can be used to treat other carbohydrate mediated diseases including cancer, viral infections, and hepatitis [5-7]. Thus, the design and development of new α-glucosidase inhibitors is a noteworthy goal for pharmacologists [8-12].

Nitrogen-containing aromatic tricyclic scaffolds such as acridine, acridone, and carbazole reveal a wide variety of biological activities including anticancer, antimicrobial, antiacetylcholinesterase, and anticonvulsant activities [13-24]. Furthermore, several natural and synthetic derivatives of the mentioned scaffolds have been reported as α-glucosidase inhibitors [25-27].

On the other hand, Wang et al. recently reported the synthesis and anti-α-glucosidase activity of a series of thioacetamide derivatives [28].

Hence, in continuation of our efforts for developing new α-glucosidase inhibitors, herein we report for the first time the synthesis of a novel series of acridine linked to thioacetamides derivatives **9a–o**, and evaluated their α-glucosidase inhibitory activity [29]. Furthermore, kinetic

study and molecular docking of synthesized compounds were also performed. Considering the numerous reports of cytotoxic effects of acridine derivatives, all synthesized compounds were evaluated by the MTT assay against breast cancer cell line MCF-7.

2. Chemistry

The pathway for the synthesis of acridine linked to thioacetamides **9a–o** has been depicted in Scheme 1. This pathway begins from the Ullmann condensation reaction of 4-methoxyaniline **1** and 2,4-dichloro-benzoic acid **2** in the presence of potassium carbonate and copper in DMF at reflux to yield 4-chloro-2-((4-methoxyphenyl)amino)benzoic acid **3**. Compound **3** easily participated in the cyclization reaction in the presence of $POCl_3$ at reflux and yeilded 6,9-dichloro-2-methoxyacridine **4**. 6,9-Dichloro-2-methoxyacridine **4** reacted with thiourea to produce 6-chloro-2-methoxyacridine-9-thiol **5** in ethanol at room temperature. On the other hand, *N*-phenyl (or benzyl)-2-chloroacetamides **8** were prepared by the reaction between amines **6** and chloroacetyl chloride **7** in DMF at room temperature. Finally, the 6-chloro-2 methoxyacridine-9-thiol **5** reacted with acetamides **8** in the presence of potassium carbonate in ethanol at reflux to provide the corresponding products **9** in good yields (80–95%).

3. Results and discussion

3.1. In vitro α-glucosidase inhibitory activity

The synthesized compounds **9a–o** were evaluated for their *in vitro* α-glucosidase inhibition potential in comparison with the marketed α-glucosidase inhibitor acarbose as a standard drug. The IC_{50} values of the two series of compounds *N*-phenylacetamide and *N*-benzylacetamide derivatives (**9a–m** and **9n–o**, respectively) are summarized in Table 1. Results revealed that all of the synthesized compounds are more potent than the standard against yeast α-glucosidase

enzyme. The most active compounds were *N*-phenylacetamide derivatives **9b**, **9f**, **9a**, and **9l** with IC_{50} values 80.0 ± 2.0, 92.2 ± 2.0, 95.0 ± 1.9, and 96.6 ± 2.0 μM, respectively. Furthermore, the remaining compounds exhibited high α-glucosidase inhibitory activities around 2–7 folds more than acarbose with the IC_{50} values ranging from 102.0 ± 1.3 to 383.1 ± 2.0 μM.

3.2. Structure–activity relationships

To study the structure–activity relationships and to optimize the anti-α-glucosidase activity of the designed scaffold, we used aniline, substituted anilines, benzyl amine, and 4-florobenzylamine to synthesize compounds **9a–o**.

In *N*-phenylacetamide derivatives series, compound **9b** with 4-methyl group on *N*-phenyl ring was found to be the most active compound among all of the synthesized compounds **9a–o**. Removal of 4-methyl group of compound **9b**, slightly reduced the inhibitory activity as observed in the third most potent compound **9a**, whereas replacement of this group with ethyl or fluorine substituents (respectively compounds **9c** and **9d**), resulted in a significant decrease in the inhibitory potential.

The inhibitory activity of the halogenated *N*-phenylacetamide derivatives against α-glucosidase demonstrated that 3-chloro*N*-phenylacetamide derivative **9f** (the second most potent) showed the most potent activity, whereas 4-fluoro derivative **9d** was the less active halo-substituted compound. The observed IC_{50} values of the chloroderivatives **9e–g** revealed that the trend of activity was 3-Cl > 3,4-dichloro > 4-Cl > 2-Cl. In addition, 4-bromo derivative **9j** exhibited more activity than its 2-bromo analog (compound **9i**). Interestingly, trend activity in the methoxy derivatives **9k–m** is similar to that in the chloro derivatives **9e–g** in the order of 3-OCH_3 > 4-OCH_3 > 2-OCH_3. These findings indicated that the interaction of synthesized compounds with α-

glucosidase enzyme, in addition to the type of substituents, is dependent on their position on the phenyl ring of *N*-phenylacetamide moiety.

Inhibitory activities of *N*-benzylacetamide derivatives **9n** and **9o** do not reveal significant difference with their corresponding *N*-phenylacetamide analogs **9a** and **9d**, respectively.

3.3. Cytotoxicity studies

Cytotoxicity of all synthesized compounds **9a–o** was evaluated against the breast cancer cell line by using MTT assay [30]. As can be seen in Table 2, the synthesized compounds did not indicate any cytotoxic activity against MCF-7 (IC_{50} > 100 μM) with the exception of compounds **9d**, **9c**, and **9n**. Compound **9d** with IC_{50} value of 13.42 ± 0.6 μM was almost as potent as the standard drug etoposide (IC_{50} = 12.4 ± 4.7 μM). To further assess of the cytotoxic effects of synthesized compounds, compounds **9d**, **9c**, and **9n** (cytotoxic compounds against MCF-7) were evaluated against the normal human cell lines HDF. Results revealed that these compounds were noncytotoxic at 100-μM concentrations to the studied normal cells.

3.4. Kinetic study

To study the mechanism of action of the synthesized compounds on α-glucosidase, a kinetic study was performed on the most potent compound **9b**. The mode of inhibition and value of K_i were determined by Lineweaver–Burk plots and secondary re-plot of these plots, respectively.

Fig. 1A shows that in the presence of various concentrations of compound **9b** the V_{max} was not affected, while the Km increased (Fig. 1A), which indicated a competitive mode of inhibition. Also, the K_i value of compound **9b** was 85 μM (Fig. 1B).

3.5. Docking study

In order to clarify the interactions of the synthesized compounds in the active site of α-glucosidase and explain the related inhibitory activities, molecular modeling studies were performed using Autodock Tools (version 1.5.6). Since, any crystallographic structure of *S.cerevisiae* α-glucosidase (used in *in vitro* assay section) do not report up-to yet, we used of the crystal structure of *S. cerevisiae* isomaltase (PDB ID: 3A4A) with 71% identity and 84% similarity toward the *S. cerevisiae* α-glucosidase for docking purpose [31]. Superimposition structure of acarbose (standard inhibitor) and most potent compound **9b** in the active site of isomaltase is presented in Figure 2.

As observed in Figure 3, acarbose interacted with the active site of isomaltase via six hydrogen bonds and one hydrophobic interaction with residues Asp69, Arg213, Glu277, Arg315, Asp352, Arg442, and Phe303.

The most active compound **9b** interacted with residues Arg315, Asp352, Arg442, Phe303, Thr306, Tyr72, Phe178, and Asp215 (Fig. 4). Phe303 and Arg315 demonstrated, respectively, π–π and π–anion interactions with acridine ring. Arg315 also made a weak hydrophobic interaction with 6-Cl substituent of acridine ring and Thr303 formed a hydrogen bond with 2-methoxy substituent of this ring. A hydrogen bond between Asp352 and NH group of compound **9b** observed. Finally, Tyr72 and Phe178, through two π–π interactions, and Asp215 and Arg442, through two π–anion interactions, interacted with the phenyl ring of the N-(4-methyphenyl)acetamide moiety.

In the second most active compound **9f**, interactions with the active site residues Glu277, Arg315, Arg442, Phe303, Tyr72, His112, Tyr158, and Phe178 were observed (Fig. 5). The acridine moiety in this compound, only through the acridine ring, interacted with active site (Phe303 and Arg315), whereas in the most potent compound, **9b**, additional interactions were

observed between the substituents of the acridine ring and the residues in the active site. In the compound **9f**, the sulfur atom showed a weak hydrophobic interaction with Tyr158. Important residues, Glu277 and Arg442, made π-anion interactions with the phenyl ring of the *N*-(3-chlorophenyl)acetamide moiety. In addition, Tyr72 formed a π–π interaction with the aforementioned ring. Furthermore, the weak hydrophobic interactions between 3-chloro substituent of the phenyl ring and the active site residues Tyr72, His112, and Phe178 were also observed.

4. Conclusion

In conclusion, the novel series of acridine linked to thioacetamide derivatives **9a–o** were designed, synthesized, and evaluated for their α-glucosidase inhibitory and cytotoxic activities. All of the target compounds revealed high α-glucosidase inhibitory activity against *S. cerevisiae* α-glucosidase (IC_{50}s < 383.1 ± 2.0 µM), when compared to acarbose as the standard drug (IC_{50} = 750.0 ± 1.5 µM). Among all the synthesized compounds, only **9d**, **9c**, and **9n** exhibited cytotoxic activity against MCF-7 cell line. In addition, kinetic analysis revealed that the most potent compound **9b** behaves as a competitive inhibitor with a K_i of 85 µM. The binding interaction of the active compounds **9b** and **9f** with the active site of enzyme was confirmed via molecular docking. This study introduced a new class of compound containing acridine moiety for the development of novel α-glucosidase inhibitors.

5. Experimental

All commercially available reagents were purchased from Merck. TLC was performed on silica gel 250 µ, F254 plates. Melting points were measured using a Kofler hot stage apparatus and are uncorrected. The IR spectra were recorded using Nicolet FT-IR Magna 550 spectrographs (KBr disks). ^{1}H and ^{1}CNMR spectra were recorded on an NMR instrument Bruker FT-500 MHz.

Elemental analyses were carried out by an Elementar Analysen system GmbH VarioEL CHN mode.

*5.1. General procedure for the synthesis of 4-chloro-2-((4-methoxyphenyl)amino)benzoic acid **3***

A solution of 4-methoxyaniline **1**(5 mmol), 2,4-dichloro-benzoic acid **2** (3 mmol), copper powder (0.2 mmol), and potassium carbonate (1.5 mmol) in DMF (30 ml) was heated under reflux for 7 h. The reaction was monitored by TLC and the product, after cooling at room temperature, was poured into hot water (1 l) and boiled in the presence of activated charcoal for 10 min. Thereafter, the obtained mixture was filtered through celite and the filtrate was acidified with HCl to obtain the precipitated product. The residue was purified using recrystallization from ethanol to obtain pure products.

*5.2. General procedure for the synthesis of 6,9-dichloro-2-methoxyacridine **4***

A mixture of 4-chloro-2-((4-methoxyphenyl)amino)benzoic acid **3** (1 mmol) and $POCl_3$(4 mmol) was heated under reflux for 3 h. After completion of reaction (checked by TLC), the reaction mixture was cooled down at room temperature, poured into crushed ice and was adjusted to alkaline pH by liquor ammonia. Thereafter, the mixture was extracted using chloroform (3 × 10 ml), washed with water, and dried over Na_2SO_4. The solvent was evaporated under reduced pressure and the residue was purified by chromatography on silica gel eluting with petroleum ether/ethyl acetate (4:1) to obtain pure products.

*5.3. General procedure for the synthesis of 6-chloro-2-methoxyacridine-9-thiol **5***

Thiourea (2 mmol) was added to a stirring solution of compound **4** (1 mmol) in ethanol (10 ml) and the reaction mixture was stirred at room temperature for 3 h. At the end of the reaction (checked by TLC), the obtained precipitate was filtered. The residue was washed with 10 ml of

water, diluted sodium bicarbonate, and diluted sodium hydroxide and was dried at 60 °C to obtain pure 6-chloro-2-methoxyacridine-9-thiol **5**.

*5.4. General procedure for the synthesis of N-phenyl (or benzyl)-2-chloroacetamide **8***

Mixture of amines **6** and chloroacetyl chloride **7** in DMF were stirred at room temperature for 30 min. At the end of the reaction (checked by TLC), the reaction mixture was diluted with water, poured into ice, and the obtained white precipitate was filtered off. The residue was washed with water to obtain pure *N*-phenyl (or benzyl)-2-chloroacetamide **8**.

*5.5. General procedure for the synthesis of acridine linked to thioacetamide **9***

A mixture of 6-chloro-2-methoxyacridine-9-thiol **5** (1 mmol), *N*-phenyl (or benzyl)-2-chloroacetamide **8** and potassium carbonate (0. 6 mmol) in acetone (10 ml) was heated under reflux for 3 h. Thereafter, the mixture was poured in cold water and was extracted using dichloromethane (4 × 10 ml), and the organic layer was dried by using Na_2SO_4. Moreover, the solvent was evaporated under reduced pressure and the residue was purified using recrystallization from ethanol to obtain the pure products (80–95%).

*5.5.1. 2-(6-chloro-2-methoxyacridin-9-ylthio)-N-phenylacetamide (**9a**)*

Pale yellow crystal; yield: 91%, Mp: 218-220 °C. IR (KBr): 3109, 2922, 1630, 1419, 1215, 811 cm^{-1}. ^1H NMR (500 MHz, DMSO-d_6): 9.84 (s, , 1H, NH), 8.675 (d, *J* =15 Hz, 1H, H8), 8.14 (s, 1H, H5), 8.035 (d, *J* =15 Hz, 1H, H7), 7.88 (s, 1H, H1), 7.62 (dd, *J* = 12.5, 5 Hz, 1H, H4), 7.48-7.51 (dd, *J* = 12.5, 5 Hz, 1H, H3), 7.16-7.21 (m, 4H, H2', H3', H5', H6'), 6.93-6.97 (m, 1H, H4'), 3.84 (s, 3H, OCH_3), 3.68 (s, 2H, CH_2S). ^{13}C NMR (100 MHz, DMSO-d_6): 166.97, 158.55, 146.91, 146.54, 139.03, 138.69, 134.43, 132.03, 130.68, 129.11, 128.87, 128.41, 127.79, 126.63, 123.99, 119.58, 102.69, 55.92. Anal. Calcd for $C_{22}H_{17}ClN_2O_2S$: C, 64.62; H, 4.19; N, 6.85. Fund: C, 64.51; H, 4.31; N, 6.68.

*5.5.2. 2-(6-chloro-2-methoxy acridine -9-ylthio)-N-p-tolylacetanide (**9b**)*

Pale yellow crystal; yield: 82%, Mp: 226-228 °C. IR (KBr): 3136, 2924, 1629, 1558, 1213, 816 cm^{-1}. ^{1}H NMR (500 MHz, DMSO-d6): 9.74 (s, , 1H, NH), 8.68 (d, J =10 Hz, 1H, H8), 8.12 (s, 1H, H5), 8.05 (d, *J* = 10 Hz, 1H, H7), 7.89 (s, 1H, H1), 7.59 (dd, *J* = 12.5, 5 Hz, 1H, H4), 7.49 (dd, *J* = 12.5, 5 Hz, 1H, H3), 7.08 (d, *J* = 10 Hz, 2H, H2', H6'), 6.95 (d, *J* = 10 Hz, 2H, H3', H5'), 3.85 (s, 3H, OCH3), 3.65 (s, 2H, CH_2S), 2.17 (s, 3H, CH3). ^{13}C NMR (100 MHz, DMSO-d6): 166.67, 158.53, 146.92, 146.56, 138.77, 136.51, 134.43, 132.89, 132.01, 129.42, 128.85, 128.41, 128.32, 126.57, 119.63, 102.71, 55.92, 20.96. Anal.Calcd for $C_{23}H_{11}ClN_2O_2S$: C, 65.32; H, 4.53; N, 6.62. Fund: C, 65.21; H, 4.69; N, 6.46.

5.5.3. 2-(6-chloro-2-methoxyacridin-9-ylthio)-N-(4-ethylphenyl)acetamide (**9c**)

Pale yellow crystal; yield: 86%, Mp: 211-215 °C. IR (KBr): 3062, 2928, 1629, 1417, 1214, 816 cm^{-1}. ^{1}H NMR (500 MHz, DMSO-d_6): 9.77 (s, , 1H, NH), 8.68 (d, *J* = 15 Hz, 1H, H8), 8.15 (d, *J* = 5 Hz, 1H, H5), 8.04 (d, *J* =15 Hz, 1H, H7), 7.89 (d, *J* = 5 Hz, 1H, H1), 7.61-7.64 (dd, *J* = 12.5, 5 Hz, 1H, H4), 7.50-7.53 (dd, *J* = 12.5, 5 Hz, 1H, H3), 7.10 (d, *J* = 10 Hz, 2H, H2', H6'), 6.99 (d, *J* = 10 Hz, 2H, H3', H5'), 3.85 (s, 3H, OCH_3), 3.68 (s, 2H, CH_2S), 2.41 (m, 2H, CH_2), 1.08 (t, *J* = 12.5 Hz, 3H, CH_3). ^{13}C NMR (100 MHz, DMSO-d_6): 166.74, 158.57, 146.92, 146.56, 139.42, 138.80, 136.72, 134.45, 132.06, 128.92, 128.42, 128.30, 127.81, 126.66, 119.69, 102.75, 55.96, 28.09, 16.20. Anal.Calcd for $C_{24}H_{21}ClN_2O_2S$: C, 65.97; H, 4.84; N, 6.41. Fund: C, 66.11; H, 4.66; N, 6.59.

5.5.4. 2-(6-chloro-2-methoxyacridin-9-ylthio)-N-(4-fluorphenyl)acetamide (**9d**)

Pale yellow crystal; yield: 91%, Mp: 200-203 °C. IR (KBr): 3064, 2103, 1630, 1517, 1215, 816 cm^{-1}. ^{1}H NMR (500 MHz, DMSO-d_6): 8.66 (d, *J* =5 Hz, 1H, NH), 8.67 (dd, *J* = 10, 5 Hz, 1H,

H8), 8.15-8.13 (m, 1H, H5), 8.01 (dd, *J* = 10, 5 Hz,1H, H7), 7.86-7.87 (m, 1H, H1), 7.63-7.59 (m, 1H, H4), 7.51-7.48 (m, 1H, H3), 7.19-7.16 (m, , 2H, H2', H6'), 7.02-6.96 (m, 2H, H3', H5'), 3.84 (s, 3H, OCH_3), 3.65 (s, 2H, CH_2S). ^{13}C NMR (100 MHz, DMSO-d_6): 166.91, 158.56, 146.91, 146.54, 138.58, 135.39, 134.43, 132.04, 130.69, 128.85, 128.42, 127.81, 126.61, 121.33, 121.25, 115.80, 115.58, 102.66, 55.944. Anal.Calcd for $C_{22}H_{16}ClFN_2O_2S$: C, 61.90; H, 3.78; N, 6.56. Fund: C, 61.78; H, 3.54; N, 6.73.

5.5.5. 2-(6-chloro-2-methoxyacridin-9-ylthio)-N-(2-chlorophenyl)acetamide (**9e**)

Pale yellow crystal; yield: 84%, Mp: 200-202 °C. IR (KBr): 3060, 2925, 1629, 1427, 1216, 816 cm^{-1}. ^1H NMR (500 MHz, DMSO-d_6): 9.43 (s, , 1H, NH), 8.69 (d, *J* =10 Hz, 1H, H8), 8.15 (d, *J* = 5 Hz, 1H, H5), 8.05 (d, *J* =10 Hz, 1H, H7), 7.88 (d, *J* = 5 Hz, 1H, H1), 7.62-7.64 (dd, *J* = 10, 5 Hz, 1H, H4), 7.52-7.55 (dd, *J* = 10, 5 Hz, 1H, H3), 7.34-7.29 (m, 2H, H3', H6'), 7.14 (m, 1H, H5'), 7.07 (m, 1H, H4'), 3.87 (s, 3H, OCH_3), 3.83 (s, 2H, CH_2S). ^{13}C NMR (100 MHz, DMSO-d_6): 167.61, 158.59, 156.32, 146.94, 146.60, 138.62, 134.80, 134.45, 132.12, 129.86, 129.00, 128.40, 127.85, 127.71, 126.84, 126.62, 126.41, 125.97, 102.81, 56.01. Anal.Calcd for $C_{22}H_{16}Cl_2N_2O_2S$: C, 59.60; H, 3.64; N, 6.32. Fund C, 59.46; H, 3.83; N, 6.56.

5.5.6. 2-(6-chloro-2-methoxyacridin-9-ylthio)-N-(3-chlorophenyl)acetamide (**9f**)

Pale yellow crystal; yield: 92%, Mp: 172-178 °C. IR (KBr): 3123, 2925, 1632, 1513, 1216, 815 cm^{-1}. ^1H NMR (500 MHz, DMSO-d_6): 9.97 (s, , 1H, NH), 8.65 (d, *J* =10 Hz, 1H, H8), 8.13 (s, 1H, H5), 8.01 (d, *J* =10 Hz, 1H, H7), 7.85 (d, *J* = 5 Hz, 1H, H1), 7.57-7.60 (dd, *J* = 10, 5 Hz, 1H, H4), 7.48 (dd, *J* = 10, 5 Hz, 1H, H3), 7.31 (s, 1H, H2'), 7.18-7.14 (m, 1H, H6'), 7.00-6.98 (m, 2H, H4', H5'), 3.85 (s, 3H, OCH_3), , 3.65 (s, 2H, CH_2S). ^{13}C NMR (100 MHz, DMSO-d_6): 167.32, 158.57, 146.92, 146.55, 140.35, 138.32, 134.43, 133.45, 132.01, 130.70, 128.77, 128.43,

127.82, 126.54, 123.67, 119.11, 117.91, 102.56, 55.87. Anal.Calcd for $C_{22}H_{16}Cl_2N_2O_2S$: C, 59.30; H, 3.64; N, 6.32. Fund: C, 59.41; H, 3.83; N, 6.19.

5.5.7. 2-(6-chloro-2-methoxyacridin-9-ylthio)-N-(4-Chlorophenyl)acetamide (**9g**)

Pale yellow crystal; yield: 80%, Mp: 224-226 °C. IR (KBr): 2923, 2853, 1628, 1466, 1213, 815 cm^{-1}. ^1H NMR (500 MHz, DMSO-d_6): 9.96 (s, , 1H, NH), 8.65 (dd, *J* =10, 5 Hz, 1H, H8), 8.14 (s, 1H, H5), 8.02 (dd, *J* =10, 5 Hz, 1H7), 7.86 (s, 1H, H1), 7.59-7.62 (m, 1H, H4), 7.51-7.48 (m, 1H, H3), 7.34-7.325(m, 2H, H2', H6'), 7.16-7.14 (m, 2H, H3', H5'), 3.85 (s, 3H, OCH_3), 3.67 (s, 2H, CH_2S). ^{13}C NMR (100 MHz, DMSO-d_6): 167.17, 158.57, 146.91, 146.54, 138.49, 138.39, 134.43, 132.07, 131.94, 130.66, 128.82, 128.43, 127.80, 126.61, 121.40, 115.59, 102.63, 55.96. Anal.Calcd for $C_{22}H_{16}Cl_2N_2O_2S$: C, 59.60; H, 3.64; N, 6.32; . Fund: C, 59.77; H, 3.81; N, 6.19.

5.5.8. 2-(6-chloro-2-methoxyacridin-9-ylthio)-N-(3,4-dichlorophenyl)acetamide (**9h**)

Pale yellow crystal; yield: 83%, Mp: 220-223 °C. IR (KBr): 3120, 2922, 1629, 1473, 1215, 812 cm^{-1}. ^1H NMR (500 MHz, DMSO-d_6): 10.03 (d, *J* = 5 Hz, 1H, NH), 8.65-8.62 (m, 1H, H8), 8.14-8.13 (m, 1H, H5), 8.02-8.00 (m, 1H, H7), 7.85-7.83 (m, 1H, H1), 7.60-7.58 (m, 1H, H4), 7.50-7.38 (m, 3H, H3, H2', H6'), 7.03-6.99 (m, 1H, H5'), 3.85 (s, 3H, OCH_3), 3.64 (s, 2H, CH_2S). ^{13}C NMR (100 MHz, DMSO-d_6): 167.50, 158.60, 146.92, 146.54, 138.97, 134.44, 132.06, 131.33, 131.03, 130.73, 128.77, 128.43, 127.85, 126.54, 120.73, 119.53, 102.55, 55.93. . Anal.Calcd for $C_{22}H_{15}Cl_3N_2O_2S$: C, 55.30; H, 3.16; N, 5.86. Fund: C, 55.47; H, 2.98; N, 5.93.

5.5.9. 2-(6-chloro-2-methoxyacridin-9-ylthio)-N-(2-bromophenyl)acetamide (**9i**)

Pale yellow crystal; yield: 86%, Mp: 203-207 °C. IR (KBr): 3131, 2957, 1629, 1511, 1215, 817 cm^{-1}. ^1H NMR (500 MHz, DMSO-d_6): 9.41 (s , 1H, NH), 8.73 (d, *J* =10 Hz, 1H, H8), 8.18 (d, *J* =5 Hz 1H, H5), 8.07 (d, *J* =10 Hz, 1H, H7), 7.92 (d, *J* = 5 Hz, 1H, H1), 7.66 (dd, *J* = 10, 5 Hz,

1H, H4), 7.56 (dd, *J* = 10, 5 Hz, 1H, H3), 7.50 (d, *J* =10 Hz, 1H, H6'), 7.23-7.17 (m, 1H, H3', H5'), 7.04-7.00 (m, 1H, H4'), 3.90 (s, 3H, OCH_3), 3.84 (s, 2H, CH_2S). ^{13}C NMR (100 MHz, DMSO-d_6): 167.49, 158.64, 147.00, 146.64, 144.48, 138.71, 136.15, 134.10, 133.10, 132.89, 132.17, 130.59, 129.52, 129.08, 128.43, 127.89, 126.67, 102.82, 56.10. Anal.Calcd for $C_{22}H_{16}BrClN_2O_2S$: C, 54.17; H, 3.31; N, 5.74. Fund: C, 54.28; H, 3.52; N, 5.59.

5.5.10. 2-(6-chloro-2-methoxyacridin-9-ylthio)-N-(4-bromophenyl)acetamide (**9j**)

Pale yellow crystal; yield: 83%, Mp: 226-228 °C. IR (KBr): 2922, 2852, 1627, 1469, 1218, 808 cm^{-1}. ^1H NMR (500 MHz, DMSO-d_6): 9.94 (s, , 1H, NH), 8.65 (d, *J* =10 Hz, 1H, H8), 8.11 (d, *J* =5 Hz, 1H, H5), 8.01 (d, *J* =10 Hz, 1H, H7), 7.86 (d, *J* = 5 Hz, 1H, H1), 7.57 (dd, *J* = 10, 5 Hz, 1H, H4), 7.48 (dd, *J* = 10, 5 Hz, 1H, H3), 7.17-7.22 (m, 4H, H2', H3', H5', H6'), 3.85 (s, 3H, OCH_3), 3.65 (s, 2H, CH_2S). ^{13}C NMR (100 MHz, DMSO-d_6): 167.08, 158.54, 146.88, 146.51, 138.52, 137.94, 134.44, 131.99, 130.68, 128.94, 128.77, 128.39, 127.80, 127.59, 126.54, 121.01, 102.60, 55.92. . Anal.Calcd for $C_{22}H_{16}BrClN_2O_2S$: C, 54.17; H, 3.31; N,5.74. Fund: C, 54.25; H, 3.48; N, 5.39.

5.5.11. 2-(6-chloro-2-methoxyacridin-9-ylthio)-N-(2-methoxyphenyl)acetamide (**9k**)

Pale yellow crystal; yield: 95%, Mp: 190-191 °C. IR (KBr):3119, 2924, 1628, 1468, 1215, 814 cm^{-1}. ^1H NMR (500 MHz, DMSO-d_6): 8.99(s, , 1H, NH), 8.65 (d, *J* =10 Hz, 1H, H8), 8.13 (d, *J* =5 Hz 1H, H5), 8.02 (d, *J* =10 Hz, 1H, H7), 7.85 (d, *J* = 5 Hz, 1H, H1), 7.60 (dd, *J* = 10, 5 Hz, 1H, H4), 7.59 (dd, *J* = 10, 5 Hz, 1H, H3),7.50 (dd, *J* = 10, 5 Hz , 1H , H6'), 7.23 (s, 1H, H3'), 6.74 (m, 2H, H4', H5'), 3.85 (s, 3H, OCH_3), 3.78 (s, 2H, CH_2S), 3.54 (s, 3H, OCH_3). ^{13}C NMR (100 MHz, DMSO-d_6): 167.16, 158.48, 147.86, 146.90, 146.54, 134.38, 131.99, 129.16, 129.04,

128.35, 128.26, 126.53, 125.20, 122.90, 111.19, 102.83, 55.92, 55.88. Anal.Calcd for $C_{23}H_{19}ClN_2O_3S$: C, 62.94; H, 4.36; N, 6.38. Fund: C, 62.81; H, 4.21; N, 6.49.

5.5.12. 2-(6-chloro-2-methoxyacridin-9-ylthio)-N-(3-methoxyphenyl)acetamide (**9l**)

Pale yellow crystal; yield: 86%, Mp: 220-224 °C. IR (KBr): 3119, 2923, 1628, 1518, 1214, 812cm^{-1}. ^{1}H NMR (500 MHz, DMSO-d_6): 9.80 (s, , 1H, NH), 8.67 (d, *J* =10 Hz, 1H, H8), 8.12-8.11 (d, *J* =5 Hz 1H, H5), 8.01 (d, *J* =10 Hz, 1H, H7), 7.89 (s, 1H, H1), 7.60-7.56 (m, 1H, H4), 7.49-7.45 (m, 1H, H3), 7.06-7.02 (m, 1H, H5'), 6.85 (d, *J* = 5 Hz, 1H, H2'), 6.73 (d, *J* = 10 Hz, 1H, H6'), 6.53-6.50 (m, 1H, H3'), 3.85 (s, 3H, OCH_3), 3.78 (s, 2H, CH_2S), 3.54 (s, 3H, OCH_3). ^{13}C NMR (100 MHz, DMSO-d_6): 166.93, 159.83, 158.53, 146.91, 146.55, 140.16, 138.64, 134.44, 131.96, 130.71, 129.78, 128.40, 128.31, 127.80, 126.55, 55.88, 55.32. Anal.Calcd for $C_{23}H_{19}ClN_2O_3S$: C, 62.94; H, 4.36; N, 6.38. Fund: C, 62.81; H, 4.21; N, 6.52.

5.5.13. 2-(6-chloro-2-methoxyacridin-9-ylthio)-N-(4-methoxyphenyl)acetamide (**9m**)

Pale yellow crystal; yield: 91%, Mp: 216-218 °C. IR (KBr): 2923, 2853, 1627, 1467, 1214, 815 cm^{-1}. ^{1}H NMR (500 MHz, DMSO-d_6): 9.65 (s, , 1H, NH), 8.68 (d, *J* =10 Hz, 1H, H8), 8.10 (d, *J* =5 Hz, 1H, H5), 8.00 (d, *J* =10 Hz, 1H, H7), 7.90 (d, *J* = 5 Hz, 1H, H1), 7.56 (dd, *J* = 10, 5 Hz, 1H, H4), 7.47 (dd, *J* = 10, 5 Hz, 1H, H3), 7.51-7.48 (m, 1H, H3), 7.08 (d, *J* = 10 Hz, 2H, H2', H6'), 6.69 (d, *J* = 10 Hz, 2H, H3', H5'), 3.86 (s, 3H, OCH_3), 3.64 (s, 3H, OCH_3), 3.62 (s, 2H, CH_2S). ^{13}C NMR (100 MHz, DMSO-d_6): 166.39, 165.23, 158.51, 155.83, 146.91, 146.55, 138.80, 134.44, 132.10, 131.93, 128.81, 128.38, 128.23, 126.50, 121.16, 114.06, 102.70, 55.89, 55.54, 40.66. Anal.Calcd for $C_{23}H_{19}ClN_2O_3S$: C, 62.94; H, 4.36; N, 6.36. Fund: C, 63.13; H, 4.51; N, 6.21.

5.5.14. 2-(6-chloro-2-methoxyacridin-9-ylthio)-N-(benzyl)acetamide (**9n**)

Pale yellow crystal; yield: 88%, Mp: 199-203 °C. IR (KBr): 3111, 2923, 1628, 1417, 1213, 819 cm^{-1}. ^{1}H NMR (500 MHz, DMSO-d_6): 8.60 (d, *J* =15 Hz, 1H, H8), 8.20 (t, *J* = 10 Hz, 1H, NH), 8.08 (d, *J* = 5 Hz, 1H, H5), 8.01 (d, *J* =10 Hz, 1H, H7), 7.85 (d, *J* = 5 Hz, 1H, H1), 7.57 (dd, *J* = 10, 5 Hz, 1H, H4), 7.51 (dd, *J* = 12.5, 5 Hz, 1H, H3), 7.13-7.05 (m, 3H, H3', H4', H5'), 6.70-6.72 (m, 2H, H2', H3'), 3.98 (d, 2H, *J* = 5 Hz, CH_2N), 3.93 (s, 3H, OCH_3), 3.57 (s, 2H, CH_2S).^{13}C NMR (100 MHz, DMSO-d_6): 168.12, 158.45, 146.64, 146.45, 138.97, 138.93, 134.39, 131.98, 130.38, 129.00, 128.59, 128.30, 128.18, 127.71, 127.45, 127.25, 126.52, 102.87, 56.09, 42.82, 39.52. Anal.Calcd for $C_{23}H_{19}ClN_2O_2S$: C, 65.32; H, 4.53; N, 6.62. Fund C, 65.51; H, 4.39; N, 6.83.

*5.5.15. N-(4-fluorobenzyl)-2-(6-chloro-2-methoxyacridin-9-ylthio)acetaide (**9o**)*

Pale yellow crystal; yield: 93%, Mp: 201-203 °C. IR (KBr):3116, 2924, 1629, 1468, 1217, 807 cm^{-1}. ^{1}H NMR (500 MHz, DMSO-d_6): 8.62 (d, *J* =10 Hz, 1H, H1), 8.23 (t, *J* =10 Hz, 1H, NH), 8.12 (d, *J* = 5 Hz, 1H, H5), 8.035 (d, *J* =15 Hz, 1H, H7), 7.87 (d, *J* = 5 Hz, 1H, H1), 7.59-7.61 (dd, *J* = 10, 5 Hz, 1H, H4), 7.52-7.55 (dd, *J* = 10, 5 Hz, 1H, H3), 6.87-6.93 (m, , 2H, H2', H6'), 6.78-6.75 (m, 2H, H3', H5'), 3.95-3.94 (m, 5H, OCH_3, CH_2S). ^{13}C NMR (100 MHz, DMSO-d_6): 168.12, 161.35 (d, J_{C-F} = 301.25 Hz), 158.49, 146.88, 146.49, 134.44, 132.03, 129.44, 129.36, 129.01, 128.33, 128.26, 126.59, 115.38, 115.17, 102.88, 56.12, 42.04. Anal.Calcd for $C_{23}H_{18}ClFN_2O_2S$: C 62.65; H, 4.11; N, 6.35. Fund C 62.76; H, 4.28; N, 6.18.

5.6. α-Glucosidase inhibition assay

Saccharomyces cerevisiae α-glucosidase (EC3.2.1.20, 20 U/mg) and substrate (p-nitrophenyl glucopyranoside) were purchased from Sigma-Aldrich. Enzyme was prepared in potassium

phosphate buffer (pH 6.8, 50 mM), and the synthesized compounds **9a–o** were dissolved in DMSO (10 % final concentration).

The various concentrations of compounds **9a-o** (20 µL), enzyme solution (20 µL), and potassium phosphate buffer (135 µL), were added in the 96-well plate and incubated at 37 °C for 10 min. Thereafter, the substrate (25 µL, 4 mM) was added to the mixture and allowed to incubate at 37 °C for 20 min. Eventually, the change in absorbance was measured at 405 nm by using spectrophotometer (Gen5, Power wave xs2, BioTek, America). DMSO as control (10 % final concentration) and acarbose as the standard drug were used. The percentage of inhibition for each entry was calculated by using the following formula:

% Inhibition = [(Abs control _ Abs sample)/Abs control] ×100

IC_{50} values were obtained from the nonlinear regression curve using the Logit method.

5.7. In vitro cytotoxicity assay

Evaluation of cytotoxic effects of the synthesized compounds **9a–o** was performed exactly based on our previous report [10].

5.8. Kinetic study

To evaluate the inhibition mode of the synthesized compound, kinetic studies were performed. The 20 µl of enzyme solution (1 U/mL) was incubated with 20 µl of various concentrations (0, 60, 80, and 100 µM) of the most potent compound **9b** for 15 min at 30 °C. The reaction was then initiated by adding different concentrations of p-nitrophenyl glucopyranoside as substrate (1–4 mM), and the change in absorbance was determined for 20 min at 405 nm by using a spectrophotometer (Gen5, Power wave xs2, BioTek, America).

5.9. Molecular docking study

Docking studies were performed using the AUTODOCK 4.2 program and the pdb structure of 3A4A was taken from the Brookhaven protein database (http://www.rcsb.org). Subsequently, the additional molecules (water molecules and the original inhibitors) were removed from the protein structure. The 3D structure of the most active compounds **9b** and **9f** were provided using MarvineSketch 5.8.3, 2012, ChemAxon (http://www.chemaxon.com). After the preparation of the autodock format of protein and selected compounds, the obtained enzyme structure was used as an input for the AUTOGRID program. AUTOGRID for each atom type in the ligand performed a precalculated atomic affinity grid maps, plus an electrostatics map and a separate desolation map presented in the ligand. All maps were calculated with 0.375 Å spacing between the grid points. The center of the grid box was placed in coordinates x = 22.6225, y = −8.069, z = 24.158. The dimensions of the active site box for all docks that were set at 50 × 50 × 50, centered at the geometrical center of co-crystallized ligand, were used. Flexible ligand dockings were accomplished for the selected ligands. Each docked system was carried out by 50 runs of the AUTODOCK search by the Lamarckian genetic algorithm (LGA). The best pose of each ligand was selected for analyzing the interactions between isomaltase and the inhibitor. The results were visualized using Discovery Studio 4.0 Client (Figs. 2–5).

Acknowledgment

The authors gratefully acknowledge the Research Council of Tehran University of Medical Sciences and Iran National Science Foundation (INSF).

Support information

References

[1] R. Rabasa-Lhoret, J.L. Chiasson, α-Glucosidase Inhibitors, International textbook of diabetes mellitus. 2004.

[2] H.S. Yee, N.T. Fong, A review of the safety and efficacy of acarbose in diabetes mellitus, Pharmacotherapy, 16(1996), 792-805.

[3] K. Yoshioka, K. Azukari, K. Ashida, Y. Kasamatsu, S. Yokoo, T. Yoshida, M. Kondo, The efficacy of voglibose on daily glycemic excursions assessed by the "J"-index in non-insulin dependent diabetes mellitus. Horm. Metab. Res. 29 (1997), 407-408.

[4] G. Pagano, S. Marena, L. Corgiat-Mansin, F. Cravero, C. Giorda, M. Bozza, C.M. Rossi, Comparison of miglitol and glibenclamide in diet-treated type 2 diabetic patients. Diabetes Metab. 21 (1995), 162-167.

[5] M.J. Humphries, K. Matsumoto, S.L. White, K. Olden, Inhibition of experimental metastasis by castanospermine in mice: blockage of two distinct stages of tumor colonization by oligosaccharide processing inhibitors, Cancer Res. 46 (1986), 5215-5222.

[6] H. Park, K.Y. Hwang, K.H. Oh, Y.H. Kim, J.Y. Lee, K. Kim, Discovery of novel α-glucosidase inhibitors based on the virtual screening with the homology-modeled protein structure, Bioorg. Med. Chem. 16 (2008), 284-292.

[7] S.J. Storr, L. Royle, C.J. Chapman, U.M.A. Hamid, J.F. Robertson, A. Murray, R.A. Dwek, P.M. Rudd, The O-linked glycosylation of secretory/shed MUC1 from an advanced breast cancer patient's serum, Glycobiology. 18 (2008), 456-462.

[8] M.T. Javid, F. Rahim, M. Taha, H.U. Rehman, M. Nawaz, S. Imran, I. Uddin, A. Mosaddik, K.M. Khan, Synthesis, in vitro α-glucosidase inhibitory potential and molecular docking study of thiadiazole analogs, Bioorg. Chem. 78 (2018), 201-209.

[9] M. Taha, S. Imran, F. Rahim, A. Wadood, K.M. Khan, Oxindole based oxadiazole hybrid analogs: Novel α-glucosidase inhibitors, Bioorg. Chem. 76 (2018), 273-280.

[10] M. Taha, S.A.A. Shah, M. Afifi, S. Imran, S. Sultan, F. Rahim, K.M. Khan, Synthesis, α-glucosidase inhibition and molecular docking study of coumarin based derivatives, Bioorg. Chem. 77 (2018), 586-592.

[11] A.A. Adegboye, K.M. Khan, U. Salar, S.A. Aboaba, S. Chigurupati, I. Fatima, M. Taha, A. Wadood, J.I. Mohammad, H. Khan, S. Perveen, 2-Aryl benzimidazoles: Synthesis, In vitro α-amylase inhibitory activity, and molecular docking study, Eur. J. Med. Chem. 150 (2018), 248-260.

[12] F. Ali, K.M. Khan, U. Salar, M. Taha, N.H. Ismail, A. Wadood, M. Riaz, S. Perveen, Hydrazinyl arylthiazole based pyridine scaffolds: Synthesis, structural characterization, in vitro α-glucosidase inhibitory activity, and in silico studies, Eur. J. Med. Chem. 138 (2017), 255-272.

[13] C. Sherer, T.J. Snape, Heterocyclic scaffolds as promising anticancer agents against tumours of the central nervous system: Exploring the scope of indole and carbazole derivatives, Eur. J. Med. Chem. 97 (2015), 552-560.

[14] F. Charmantray, A. Martelli, Interest of acridine derivatives in the anticancer chemotherapy, Curr. Pharm. Des. 7(2001), 1703-1724.

[15] M. Mohammadi-Khanaposhtani, M. Safavi, R. Sabourian, M. Mahdavi, M. Pordeli, M. Saeedi, S.K. Ardestani, A. Foroumadi, A. Shafiee, T. Akbarzadeh, Design, synthesis, in vitro cytotoxic activity evaluation, and apoptosisinduction study of new 9 (10H)-acridinone-1, 2, 3-triazoles, Mol. Divers. 19 (2015) 787–795.

[16] W. Gu, S. Wang, Synthesis and antimicrobial activities of novel 1H-dibenzo [a, c] carbazoles from dehydroabietic acid, Eur. J. Med. Chem. 45(2010), 4692-4696.

[17] N.K. Ladani, D.C. Mungra, M.P. Patel, R.G. Patel, Microwave assisted synthesis of novel Hantzsch 1, 4-dihydropyridines, acridine-1, 8-diones and polyhydroquinolines bearing the tetrazolo [1, 5-a] quinoline moiety and their antimicrobial activity assess, Chin. Chem. Lett. 22(2011), 1407-1410.

[18] J. Salimon, N. Salih, E. Yousif, A. Hameed, A. Kreem, Synthesis and pharmacological evaluation of 9 (10H)-acridone bearing 1, 3, 4-oxadiazole derivatives as antimicrobial agents, Arab. J. chem. 3(2010), 205-210.

[19] N.S. Kumar, P.K. Mukherjee, S. Bhadra, B.P. Saha, B.C. Pal, Acetylcholinesterase inhibitory potential of a carbazole alkaloid, mahanimbine, from Murraya koenigii, Phytother. Res. 24(2010), 629-631.

[20] S. Hamulakova, L. Janovec, O. Soukup, D. Jun, K. Kuca, Synthesis, in vitro acetylcholinesterase inhibitory activity and molecular docking of new acridine-coumarin hybrids, Int. J. Biol. Macromol. 104 (2017), 333-338.

[21] M. Mohammadi-Khanaposhtani, M. Mahdavi, M. Saeedi, R. Sabourian, M. Safavi, M. Khanavi, A. Foroumadi, A. Shafiee, T. Akbarzadeh, Design, Synthesis, biological evaluation,

and docking study of acetylcholinesterase inhibitors: new acridone-1, 2, 4-oxadiazole-1, 2, 3-triazole hybrids, Chem. Biol. Drug Des. 86 (2015) 1425–1432.

[22] M. Mohammadi-Khanaposhtani, M. Saeedi, M. Mahdavi, N.S. Zafarghandi, R. Sabourian, E.K. Razkenari, H. Alinezhad, M. Khanavi, A. Foroumadi, A. Shafiee, T. Akbarzadeh, Potent acetylcholinesterase inhibitors: design, synthesis, biological evaluation, and docking study of acridone linked to 1, 2, 3-triazole derivatives, Eur. J. Med. Chem. 92 (2015) 799–806.

[23] S.K. Srivastava, S. Srivastava, S.D. Srivastava, Synthesis of new carbazolyl thiadiazol-2-oxo-azetidines: Antimicrobial, anticonvulsant and anti-inflammatory agents, (1999)

[24] M. Mohammadi-Khanaposhtani, M. Shabani, M. Faizi, I. Aghaei, R. Jahani, Z. Sharafi, N.S. Zafarghandi, M. Mahdavi, T. Akbarzadeh, S. Emami, A. Shafiee, A. Foroumadi, Design, synthesis, pharmacological evaluation, and docking study of new acridone-based 1, 2, 4-oxadiazoles as potential anticonvulsant agents, Eur. J. Med. Chem. 112 (2016) 91–98.

[25] Z. Toobaei, R. Yousefi, F. Panahi, S. Shahidpour, M. Nourisefat, M.M. Doroodmand, A. Khalafi-Nezhad, Synthesis of novel poly-hydroxyl functionalized acridine derivatives as inhibitors of α-glucosidase and α-amylase. Carbohydr. Res. 411 (2015), 22-32.

[26] P.H. Dang, T.H. Le, P.K. Phan, P.T. Le, M.T. Nguyen, N.T. Nguyen, Two acridones and two coumarins from the roots of Paramignya trimera. Tetrahedron Lett. 58 (2017), 1553-1557.

[27] (a)H.D. Deng, W.L. Mei, H. Wang, Z.K. Guo, W.H. Dong, H. Wang, S.P. Li, H.F. Dai, Carbazole alkaloids from the peels of Clausena lansium, J. Asian Nat. Prod. Res. 16 (2014), 1024-1028. (b) G. Wang, J. Wang, D. He, X. Li, J. Li, Z. Peng, Synthesis and biological evaluation of novel 1, 2, 4-triazine derivatives bearing carbazole moiety as potent α-glucosidase inhibitors, Bioorganic Med. Chem. Lett. 26 (2016), 2806-2809. (c) C. Uvarani, M. Sankaran, N.

Jaivel, K. Chandraprakash, A. Ata, P.S. Mohan, Bioactive dimeric carbazole alkaloids from Murraya koenigii. J. Nat. Prod. 76 (2013), 993-1000.

[28] G. Wang, X. Li, J. Wang, Z. Xie, L. Li, M. Chen, S. Chen, Y. Peng, Synthesis, molecular docking and α-glucosidase inhibition of 2-((5, 6-diphenyl-1, 2, 4-triazin-3-yl) thio)-N-arylacetamides. Bioorganic Med. Chem. Lett. 27 (2017), 1115-1118.

[29] H. Nikookar, M. Mohammadi-Khanaposhtani, S. Imanparast, M.A. Faramarzi, P.R. Ranjbar, M. Mahdavi, B. Larijani, Design, synthesis and in vitro α-glucosidase inhibition of novel dihydropyrano[3,2-c]quinoline derivatives as potential anti-diabetic agents, Bioorg. Chem. 77 (2018) 280-286.

[30] T.J. Mosmann, Rapid colorimetric assay for cellular growth and survival: application to proliferation and cytotoxicity assays, Immunol. Methods. 65 (1983) 55-63.

[31] H. Sun, W. Ding, X. Song, D. Wang, M. Chen, K. Wang, Y. Zhang, P. Yuan, Y. Ma, R. Wang, R.H. Dodd, Synthesis of 6-hydroxyaurone analogues and evaluation of their α-glucosidase inhibitory and glucose consumption-promoting activity: Development of highly active 5, 6-disubstituted derivatives. Bioorganic Med. Chem. Lett. 27 (2017), 3226-3230.

Captions:

Fig. 1. Kinetics of α-gluosidase inhibition by **9b**. (a) The Lineweaver– Burk plot in the absence and presence of different concentrations of **9b** (μM); (b) the secondary plot between K_m and various concentrations of **9b**.

Fig. 2. Superimposition of the most potent compound **9b** (pink) and acarbose (cyan) in the active site of enzyme.

Fig. 3. Docking pose of acarbose in the active site of enzyme.

Fig. 4. Docking pose of the compound **9b** in the active site of enzyme.

Fig. 5. Docking pose of the compound **9f** in the active site of enzyme.

Scheme 1. Synthesis of compounds **9**. Reagents and conditions:**:** (a) K_2CO_3, Cu, DMF, reflux ,7h, (b) $POCl_3$, reflux, 3 h, (c) Thiourea, EtOH, r.t, 1 h, (d) r.t, 30 min, and (e) EtOH, K_2CO_3, reflux, 2h.

Table 1

In vitro α-glucosidase inhibitory activity of compounds **9a–o**.

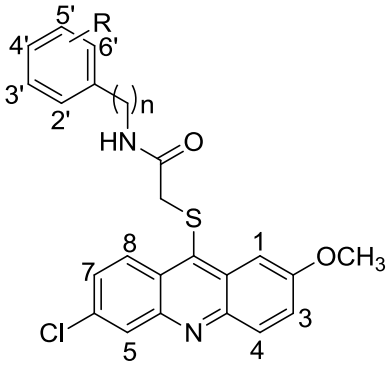

Compound	n	R	IC_{50} (μM) [a]
9a	0	H	95.0 ± 1.9
9b	0	4-CH3	80.0 ± 2.0
9c	0	4-CH2CH3	129.5 ± 2.0
9d	0	4-F	241.0 ± 1.7
9e	0	2-Cl	195.0 ± 1.2
9f	0	3-Cl	92.2 ± 2.0
9g	0	4-Cl	144.2 ± 1.1
9h	0	3,4-dichloro	102.0 ± 1.3
9i	0	2-Br	173.4 ± 1.6
9j	0	4-Br	118.2 ± 2.0
9k	0	2-OCH3	383.1 ± 2.0
9l	0	3-OCH3	96.6 ± 2.0
9m	0	4-OCH3	147.0 ± 1.5
9n	1	H	118.3 ± 1.7
9o	1	F	220.0 ± 1.5
Acarbose	-	-	750.0 ± 1.5

[a] Data are expressed as mean ± S.E. of at least three different experiments.

Table 2

Cytotoxicity evaluation of compounds **9a-o**

Compound	MCF-7 (IC_{50} μM)[a]	Compound	MCF-7 (IC_{50} μM)[a]
9a	>100	**9i**	>100
9b	>100	**9j**	>100
9c	26.59 ± 1.3	**9k**	>100
9d	13.42 ± 0.6	**9l**	>100
9e	>100	**9m**	>100
9f	>100	**9n**	55.23 ± 0.8
9g	>100	**9o**	>100
9h	>100	**Etoposide**	12.4 ± 4.7

[a] Data are expressed as mean ± S.E. of at least three different experiments.

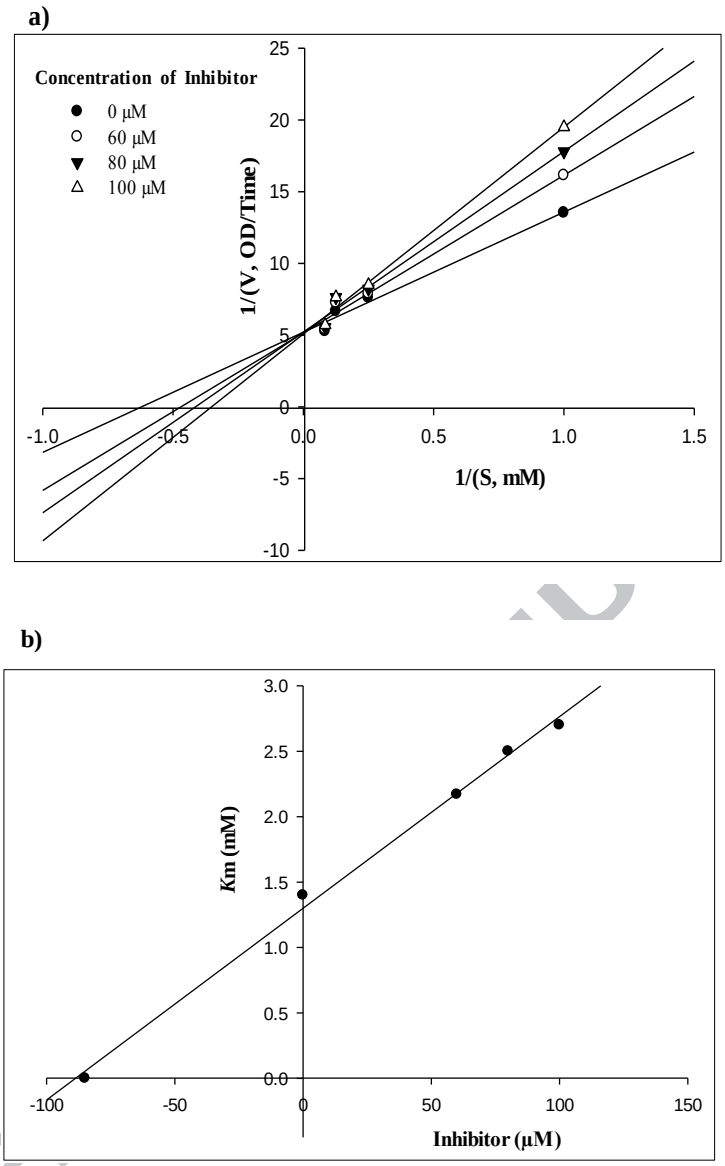

Fig. 1. Kinetics of α-gluosidase inhibition by **9b**. (a) The Lineweaver– Burk plot in the absence and presence of different concentrations of **9b** (µM); (b) the secondary plot between K_m and various concentrations of **9b**.

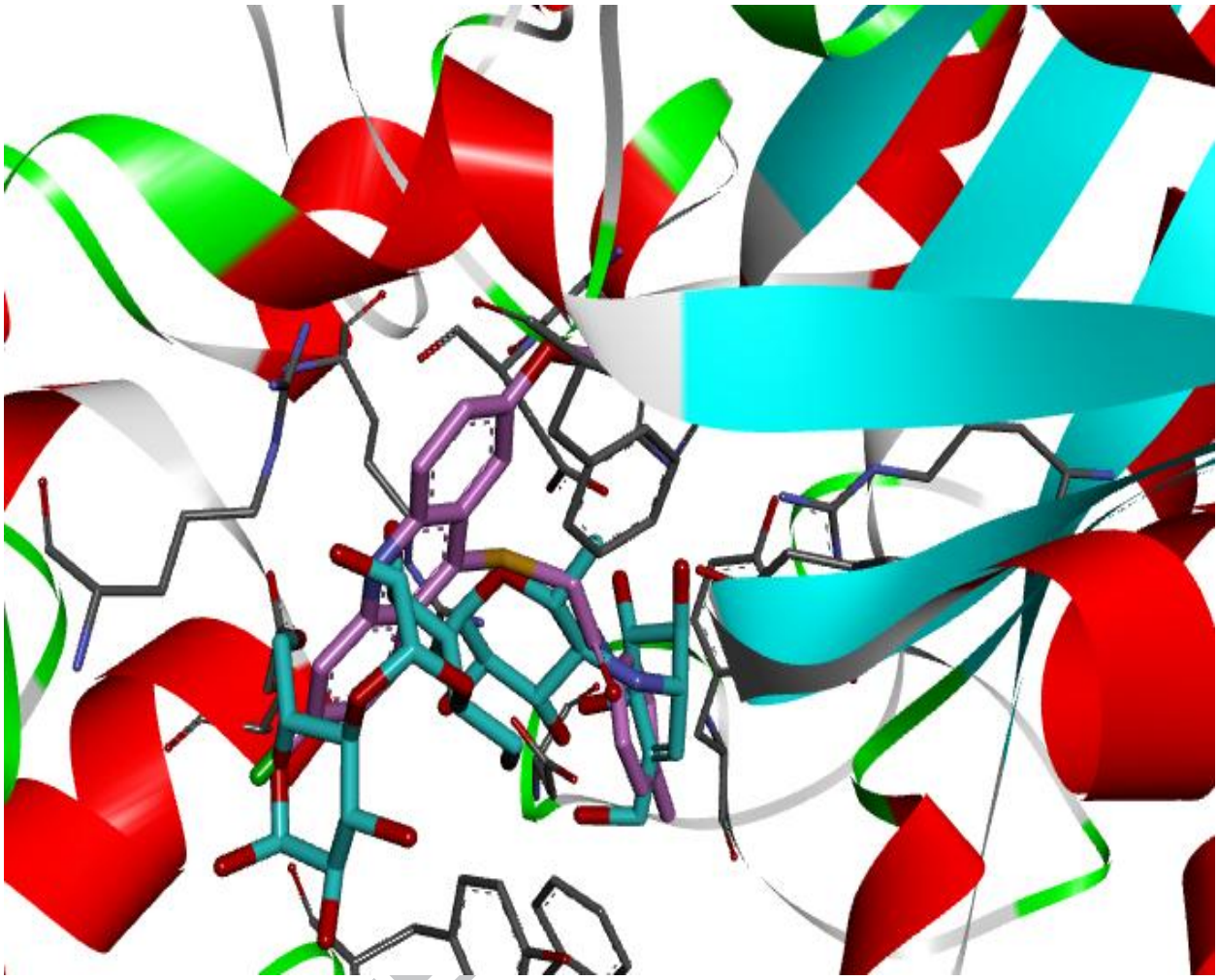

Fig. 2. Superimposition of the most potent compound **9b** (pink) and acarbose (cyan) in the active site of enzyme.

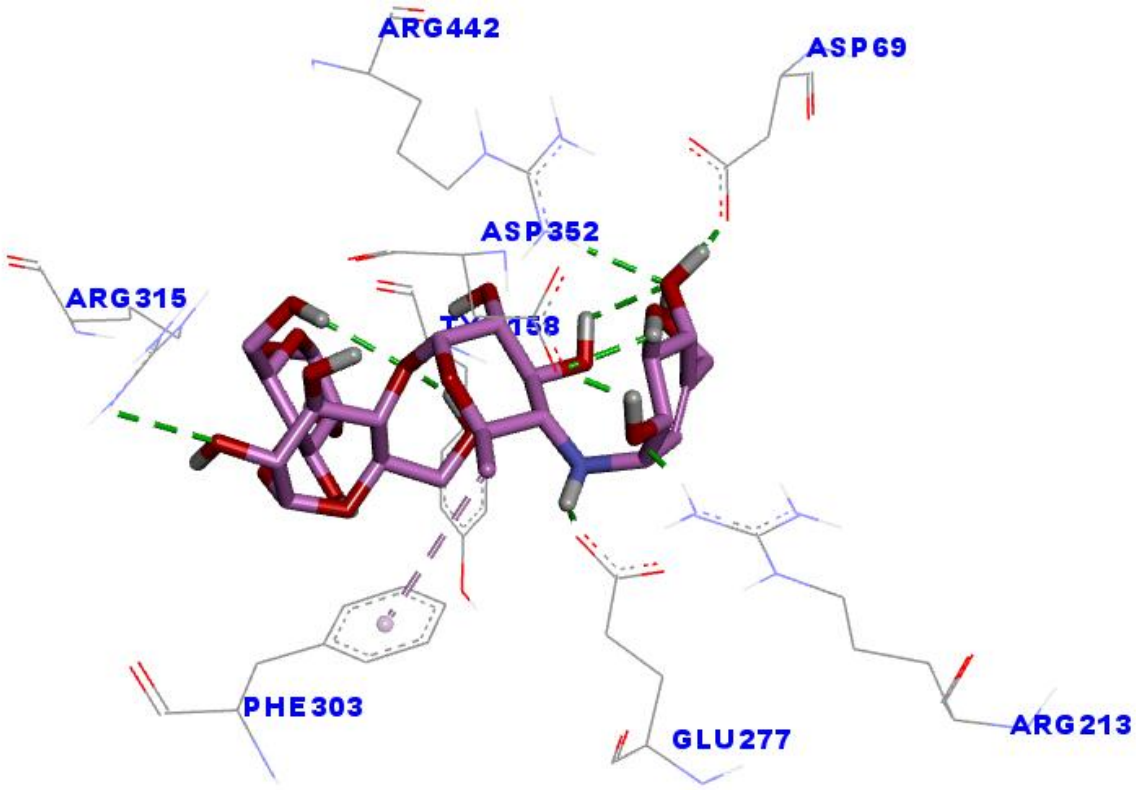

Fig. 3. Docking pose of acarbose in the active site of enzyme.

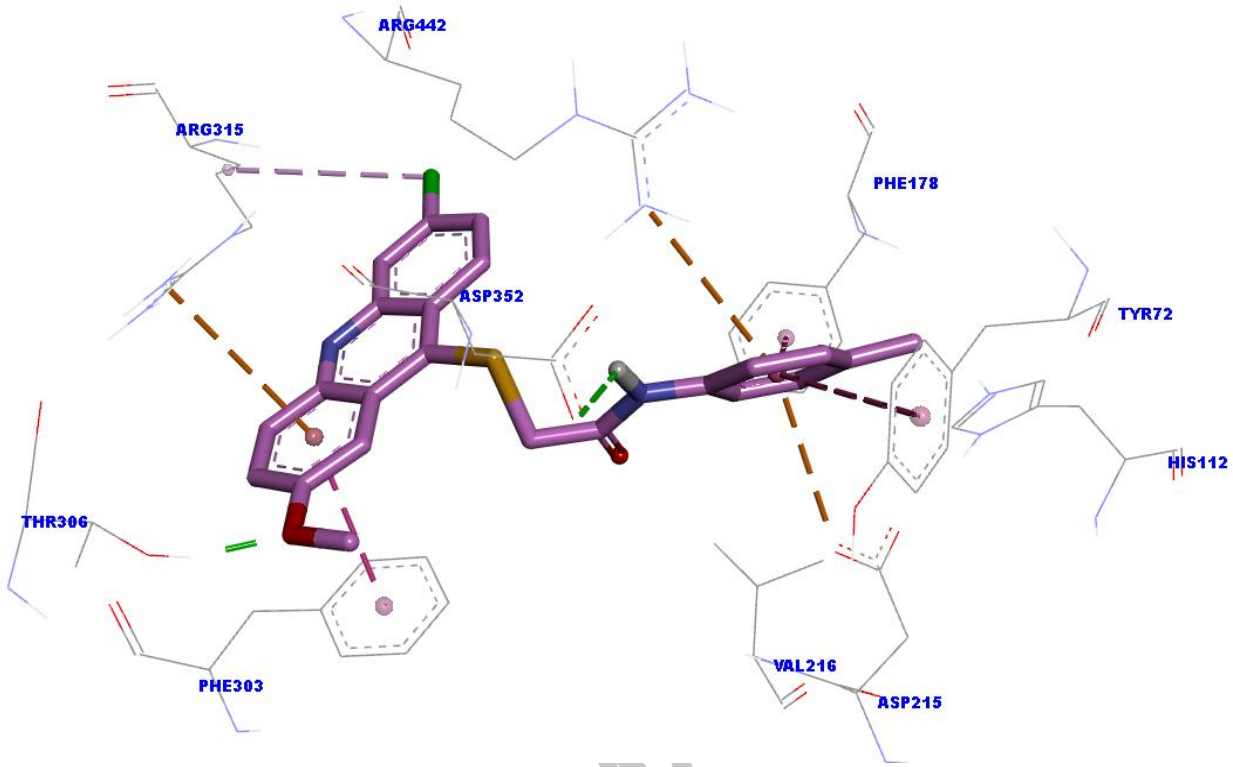

Fig. 4. Docking pose of the compound **9b** in the active site of enzyme.

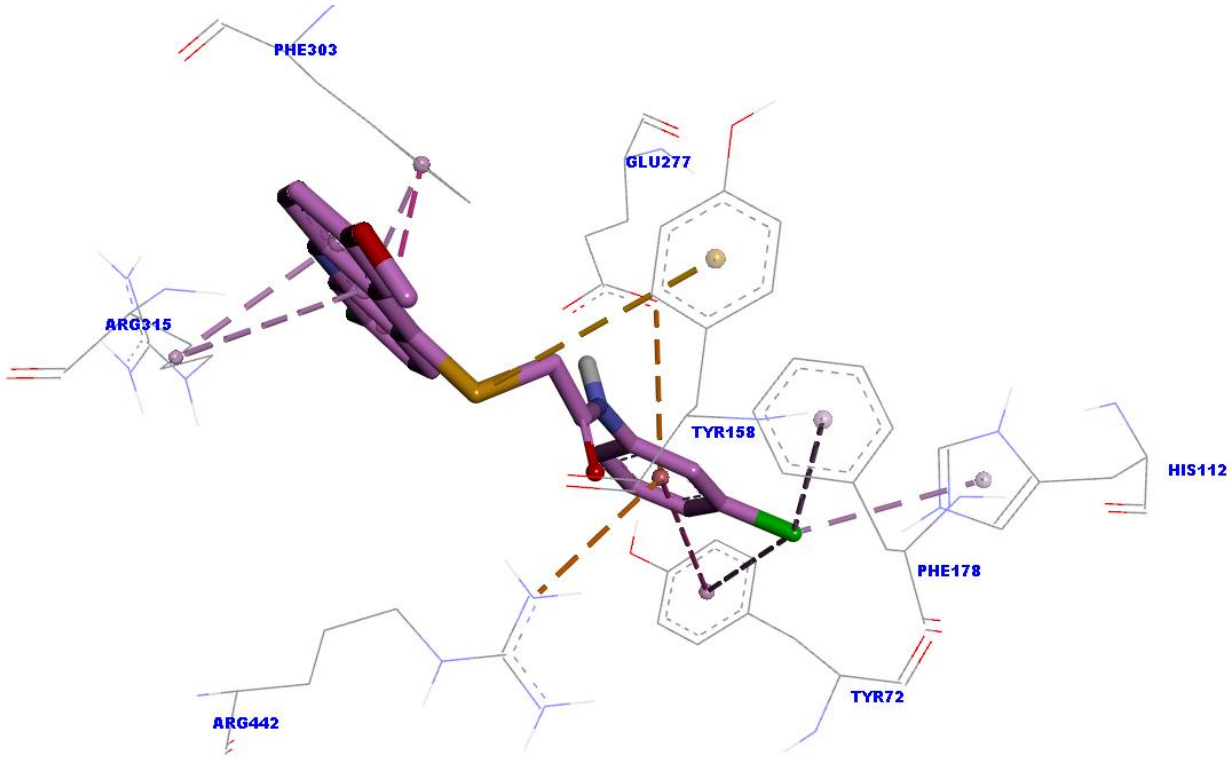

Fig. 5. Docking pose of the compound **9f** in the active site of enzyme.

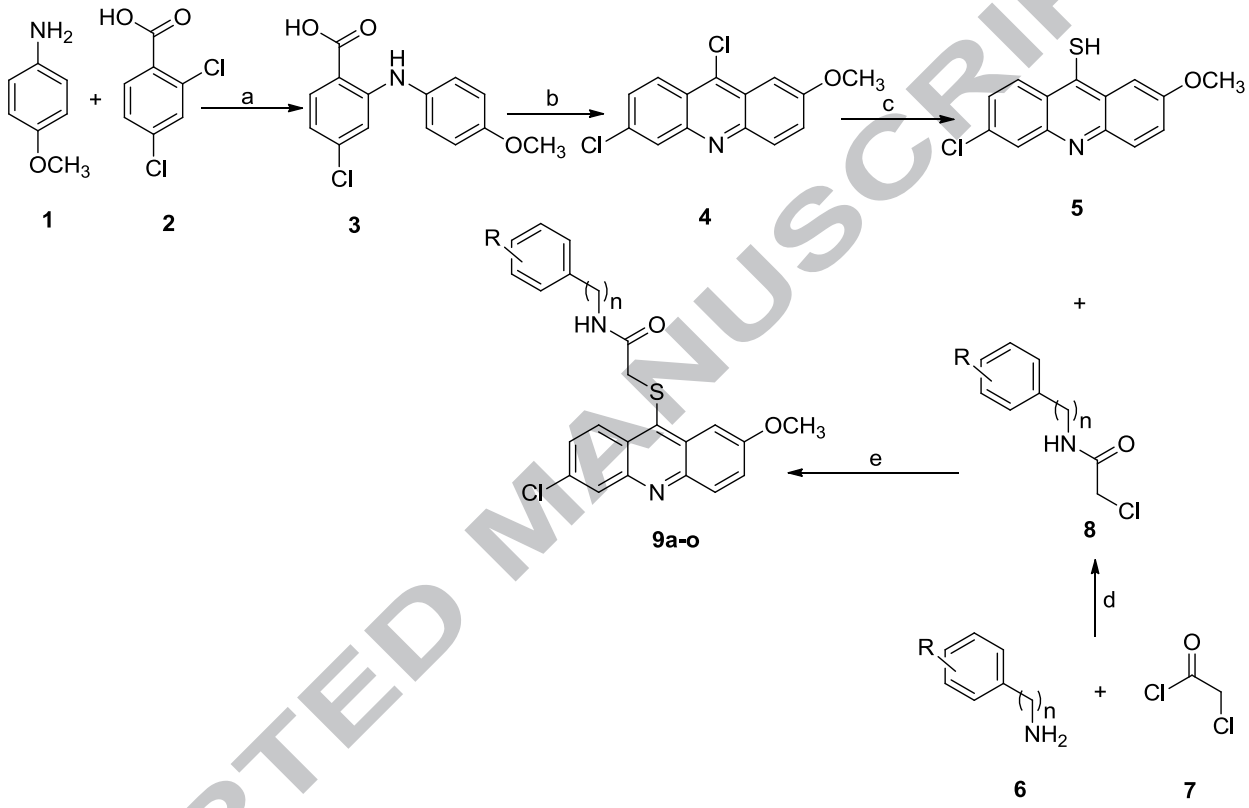

Scheme 1. Synthesis of compounds **9**. Reagents and conditions:**:** (a) K_2CO_3, Cu, DMF, reflux ,7h, (b) $POCl_3$, reflux, 3 h, (c) Thiourea, EtOH, r.t, 1 h, (d) r.t, 30 min, and (e) EtOH, K_2CO_3, reflux, 2h.

Highlights

- A novel series of acridine linked to thioacetamides **9a-o** were synthesized as α-glucosidase inhibitors.
- All the compounds showed more inhibitory activity of than standard drug acarbose
- Compound **9b** was the most potent compound with inhibitory activity around 11.7 fold more than acarbose.

The molecular modeling study permitted us to predict binding mode of synthesized compounds in active site of α-glucosidase.

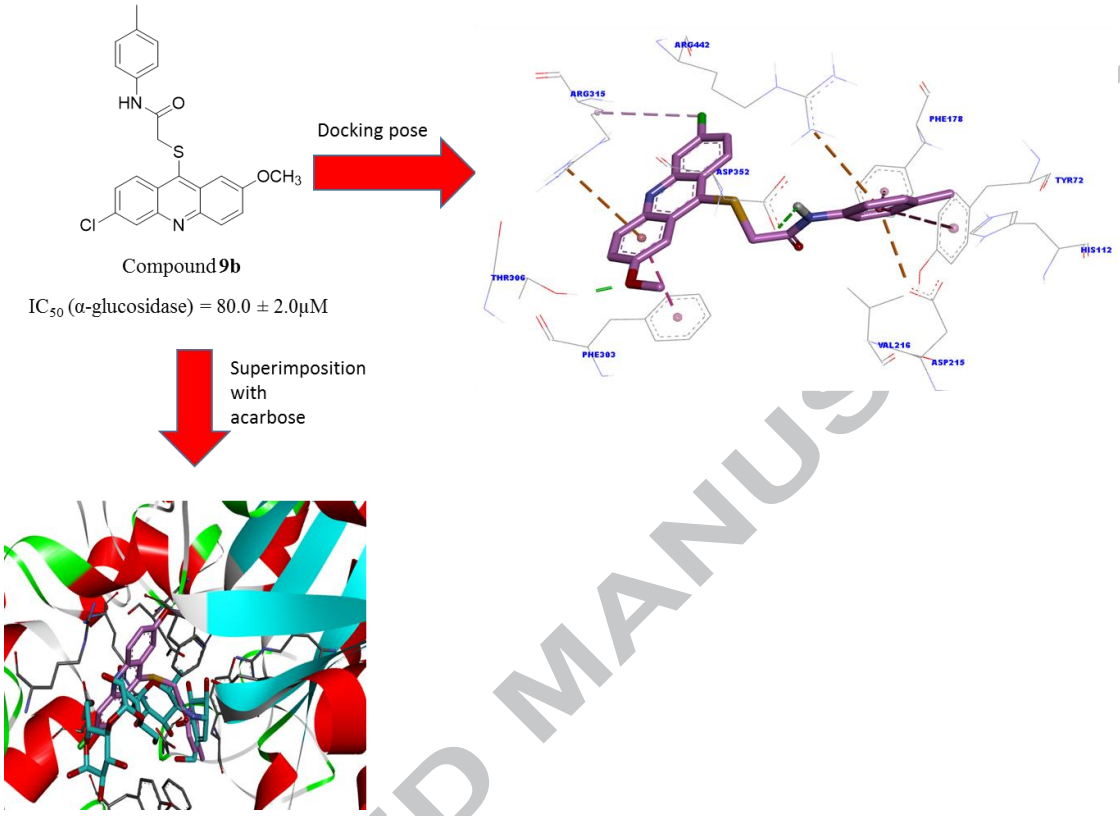

A new series of acridine linked to thioacetamides **9a-o** were synthesized and evaluated as novel inhibitors for α-glucosidase. All the compounds showed more inhibitory activity of than standard drug acarbose, and also with exception the compounds **9d**, **9c**, and **9n** found to be non-cytotoxic. The compound **9b** showed the most potent anti-α-glucosidase activity (IC_{50} value = 80.0 ± 2.0 μM). Furthermore, the interaction modes of the most potent compounds **9b** and **9f** with α-glucosidase was evaluated through molecular docking studies.